nature geoscience

LETTERS

PUBLISHED ONLINE: 5 JULY 2009 | DOI: 10.1038/NGEO574

Considerable methane fluxes to the atmosphere from hydrocarbon seeps in the Gulf of Mexico

Evan A. Solomon[1]*, Miriam Kastner[1], Ian R. MacDonald[2] and Ira Leifer[3]

The fluxes of the greenhouse gas methane from many individual sources to the atmosphere are not well constrained[1]. Marine geological sources may be significant[2], but they are poorly quantified and are not included in the Intergovernmental Panel on Climate Change budget[1]. Previous results based on traditional indirect sampling techniques and modelling suggested bubble plumes emitted from marine seeps at depths greater than 200 m do not reach the surface mixed layer because of bubble dissolution and methane oxidation[3–5]. Here we report methane concentration and isotope-depth profiles from direct submersible sampling of deepwater (550–600 m) hydrocarbon plumes in the Gulf of Mexico. We show that bubble size, upwelling flows and the presence of surfactants inhibit bubble dissolution, and that methane oxidation is negligible. Consequently, methane concentrations in surface waters are up to 1,000 times saturation with respect to atmospheric equilibrium. We estimate that diffusive atmospheric methane fluxes from individual plumes are one to three orders of magnitude greater than estimates from shallow-water seeps[6–8], greatly expanding the depth range from which methane seep emissions should be considered significant. Given the widespread occurrence of deepwater seeps, we suggest that current estimates of the global oceanic methane flux to the atmosphere[1] may be too low.

Hydrocarbon seeps are ubiquitous along continental margins, and hydrocarbon gas is emitted to the water column as bubble plumes from focused vents within the larger seep sites (see Supplementary Fig. S1). Progress in quantifying CH_4 emissions has been restricted by difficulties in sampling the bubble plumes with traditional techniques. In the Gulf of Mexico (GOM), bubble plumes are commonly visible throughout the water column on echograms[9] (Fig. 1a), and the bubbles are often coated with a thin oil layer[10]. On reaching the sea surface (Fig. 1b), this oil is detected by satellite remote sensing methods such as synthetic aperture radar (SAR; refs 9, 11). SAR imagery shows ~350 perennial oil slicks associated with plumes offshore Louisiana[9,11,12] (see Supplementary Fig. S2), and ~100 slicks in the southern GOM (refs 12, 13). These are conservative estimates that exclude non-oily plumes, which may be as abundant as oily ones[9,10].

Traditionally, shipboard hydrocasts have been used to sample the water column over seeps; however, they are ineffective at targeting seafloor vents and bubble plumes. Hence, we used a submersible to collect water-column samples immediately adjacent to six bubble plumes from the seafloor vents to the sea surface during two research expeditions. Navigation through the water column was based on visual identification of gas bubbles during ascent.

The extent of CH_4 consumption by aerobic oxidation in the water column and the atmospheric methane flux from six plumes were assessed at three GOM seep sites from depths of ~550 to 600 m (Fig. 1c). Sites GC 185 and GC 234 are seeps containing gas hydrate outcrops that breach the sea floor. Perennial bubble plumes escape from gas vents within and adjacent to the outcrops. GB 425 is a mud volcano at ~600 m depth. Hydrocarbons are discharged in a steady stream from its centre, and the bubbles are not oily[9,10].

Bottom waters sampled by submersible have CH_4 concentrations ranging from 124 to 13,660 nM (Fig. 2b). Bottom water collected by hydrocasts adjacent to the bubble plumes and at background

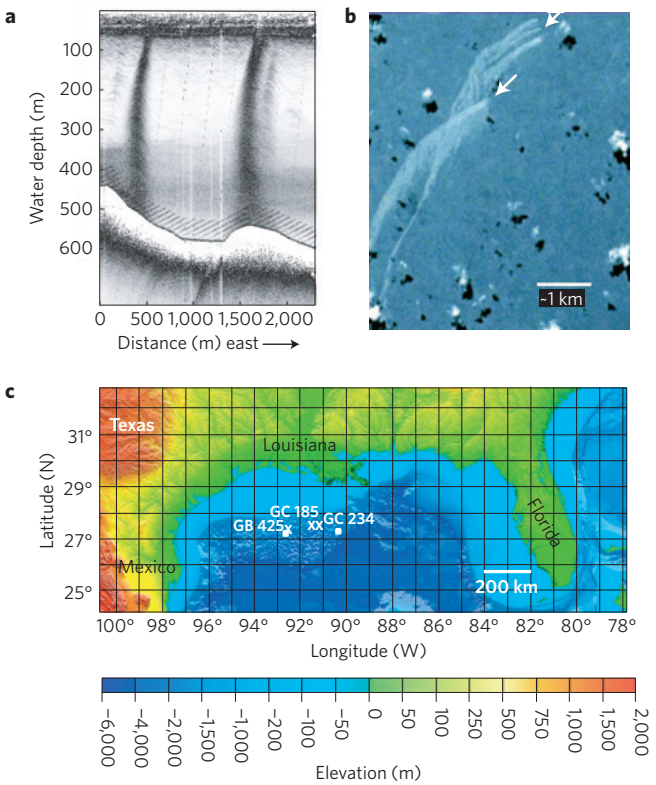

Figure 1 | Perennial hydrocarbon plumes and their associated sea-surface oil footprints. a, East–west trace of a 10 kHz echo-sounder showing two bubble plumes at GC 185. Figure from ref. 9. **b**, Photograph from a space shuttle showing that the bubble oil coating reaches the sea surface in distinct footprints (arrows), forming perennial oil slicks above the plumes. Figure from ref. 11. **c**, Bathymetric map of the northern GOM. Crosses are the locations of the hydrocarbon seep sites examined in this study and circles are the locations of nearby wind-recording stations. Bathymetry from the NOAA National Geophysical Data Center.

[1]Scripps Institution of Oceanography, University of California, San Diego, 9500 Gilman Drive #0212, La Jolla, California 92093-0212, USA, [2]Physical and Life Sciences Department, Texas A&M University-Corpus Christi, 6300 Ocean Drive, Corpus Christi, Texas 78412, USA, [3]Marine Science Institute, University of California, Santa Barbara, California 93106, USA. *e-mail: esolomon@ucsd.edu.

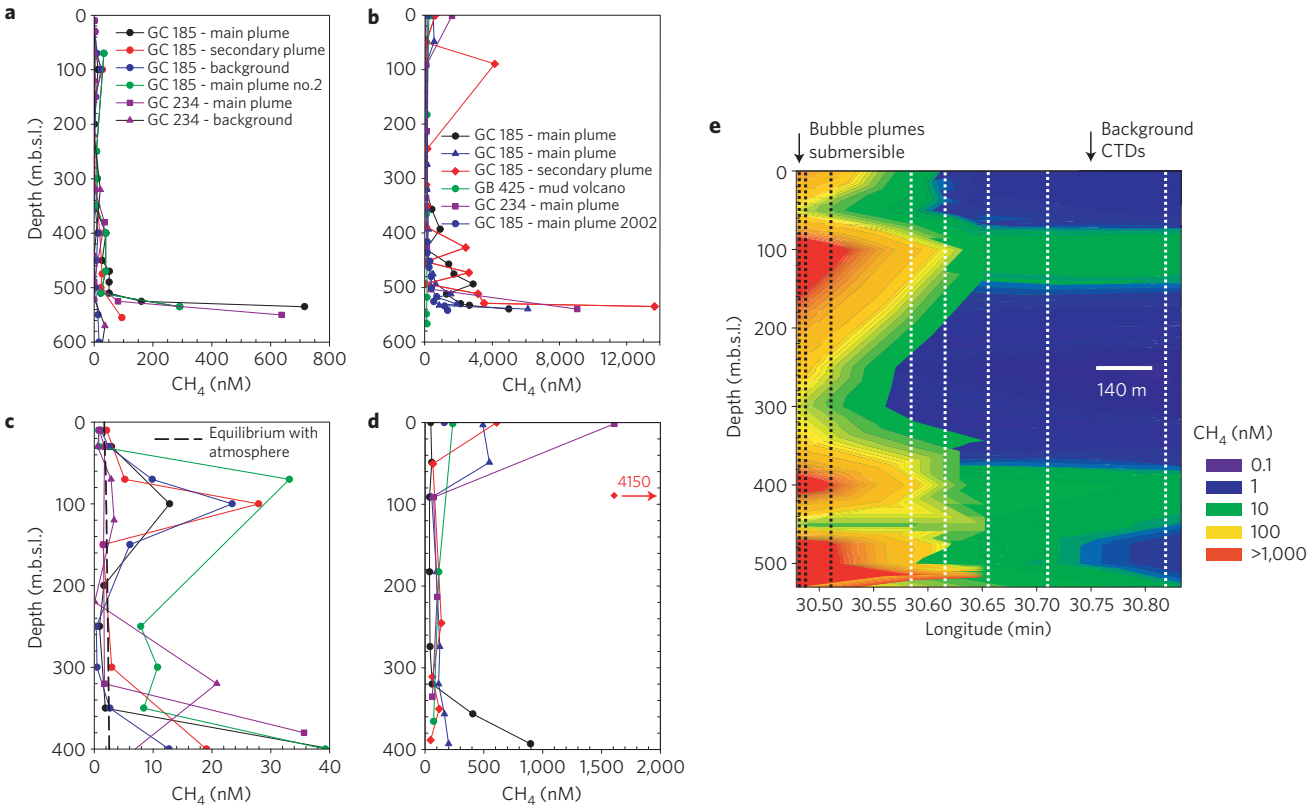

Figure 2 | Methane concentration profiles sampled by hydrocast and submersible. a, Methane concentrations from traditional CTD casts. **b**, Methane concentrations sampled by submersible. Note the concentration scale is expanded with respect to **a**. **c**, Methane concentrations from CTD casts in the upper water column. **d**, Methane concentrations sampled by submersible in the upper water column. Note the concentration scale is expanded with respect to **c**. **e**, Two-dimensional contour plot of the water-column CH_4 distribution at GC 185. The plot is based on three submersible dives and five hydrocasts represented as black and white dotted lines, respectively. Standard error = ±2%.

sites >400 m from the plumes had concentrations ~12% of those sampled by submersible (Fig. 2a). Methane concentrations sampled by submersible in the plumes decrease by 80–99% from the sea floor to 350 m water depth, are relatively constant between 350 and 80 m, then increase near the sea surface up to 1,609 nM in both the oily and non-oily plumes (Fig. 2c,d). These exceptionally high CH_4 concentrations coincide with the mixed layer, where CH_4 sea-to-air evasion is faster than microbial oxidation[3].

The bottom-water $\delta^{13}C$–CH_4 ranges from −54.4 to −44.7‰ (Fig. 3a,b). An increase in $\delta^{13}C$–CH_4 from the sea floor to the surface indicates the occurrence and extent of microbial methane oxidation if mixing with background sea water is negligible (see Supplementary Discussion). There is only a minor increase in $\delta^{13}C$–CH_4 from the sea floor to the surface in plumes sampled by submersible, but there is an 18‰ enrichment in one conductivity–temperature–depth (CTD) cast (Fig. 3a,b). An open-system, oxidation model[14] was used to estimate the fraction of the CH_4 input flux oxidized in the plumes from the $\delta^{13}C$–CH_4 profiles. The model shows that only 0–37% of the input flux is oxidized in the samples collected by submersible from both oily and non-oily plumes. A significant portion of dissolved CH_4 that escapes oxidation is transported to the mixed layer with the bubbles. Using the same model for the CTD cast data, 3–97% of the CH_4 not transported upwards with the bubbles is oxidized (Table 1).

Previous studies at other basins have indicated that bubble-plume CH_4 emanating from water depths >200 m does not reach the mixed layer because of bubble dissolution and oxidation during ascent[3–5]. Our data and the natural oil slicks at the sea surface indicate that bubble plumes do reach the mixed layer in the GOM (refs 11–13). At all GOM sites, the oil surfacing

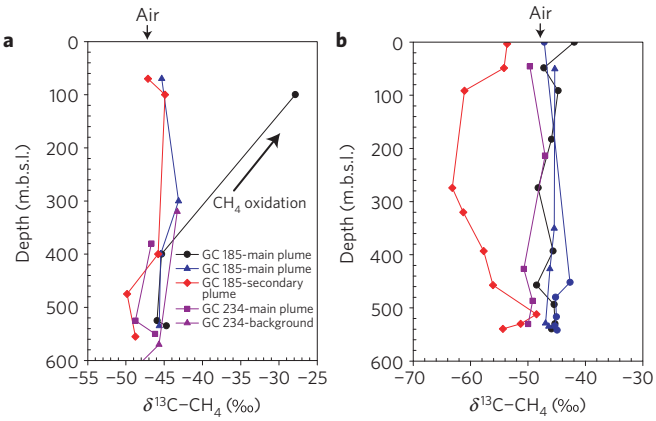

Figure 3 | Water-column $\delta^{13}C$-CH_4 profiles from the plumes sampled by CTD casts and submersible. a, Water-column $\delta^{13}C$-CH_4 from CTD casts. An increase in $\delta^{13}C$-CH_4 from the sea floor to sea surface indicates aerobic methane oxidation. **b**, $\delta^{13}C$-CH_4 depth profiles sampled by submersible showing only minor aerobic methane oxidation within the water column. Standard error = ±0.6‰.

footprints are laterally within ~200–1,000 m from the seafloor vents[11]. For the oil to surface this close to the vents requires bubble-mediated seafloor (~550 m) to sea-surface transport with velocities of 10–50 cm s^{-1} (assuming lateral currents of ~20 cm s^{-1}); oil droplets alone are insufficiently buoyant to rise at this speed[11] (for example, a 1 cm oil droplet rises at 1 cm s^{-1}). The bubble plumes studied in the GOM have high bubble fluxes, upwelling

Table 1 | Water-column CH_4 oxidation and mixed-layer diffusive CH_4 fluxes to the atmosphere.

Plume experiments	Mixed-layer CH_4 (nM)	Times saturation*	% Input flux oxidized†	Contemporary flux‡ (μmol CH_4 m^{-2} d^{-1})		
				Average	Minimum	Maximum
Submersible sampling						
GC 185 main plume	57.1	30	37	566	313	895
GC 185 main plume	492	288	8	2,770	2,220	3,370
GC 185 secondary plume	608	354	11	3,420	2,750	4,160
GB 425 mud volcano	236	137	—	197	61.9	399
GC 234 main plume	1,609	954	3	6,520	3,470	10,500
GC 185 main plume 2002	164	96	0	362	117	736
CTDs						
GC 185 main plume	2.92	1.5	97	7.0	5.6	8.5
GC 185 main plume	0.760	0.40	3	−0.38	−0.04	−1.0
GC 185 main plume	2.10	1.2	16	4.2	2.3	6.7
GC 185 background	1.13	0.66	—	−0.12	−0.01	−0.35
GC 185 background	1.71	1.0	—	0.01	0	0.03
GC 234 main plume	1.75	1.0	—	0.05	0.02	0.11
GC 234 background	0.880	0.52	—	−0.29	−0.04	−0.77

*Computed from the observed concentration of CH_4 divided by the CH_4 in sea water equilibrated with ambient air at *in situ* conditions[27]. Average CH_4 in air = 1.77403 ppmv (ref. 1).

†Water-column $\delta^{13}C$–CH_4 profiles that lacked adequate sample density were not used to compute per cent oxidation and are indicated with a dash.

‡Fluxes calculated from the range in gas transfer coefficients based on the average daily wind speed $\pm 1\sigma$ presented in Supplementary Table S2.

flows and broad bubble-size distributions that extend to large bubbles, with bubbles commonly oil-coated, all of which are critical factors that enhance bubble-mediated CH_4 transport to the sea surface[11,15]. Using a simplified bubble propagation model for bubbles at GC 185, it was predicted[11] that only oily bubbles >4.5 mm radius would reach the sea surface (see Supplementary Fig. S3). Using an improved version of the model that considers depth-dependent compressibility, solubility and hydrate skin effects within the hydrate stability field[16], as well as upwelling flows, we show that non-oily bubbles with an initial radius of ~2.4–6 mm at these and similar GOM sites as well reach the mixed layer from 550 m depth (see Supplementary Methods, Fig S4).

We propose that the loss of 80–99% of the plume CH_4 between the sea floor and 350 m and the increase in CH_4 concentrations above ~80 m (Fig. 2b) is a manifestation of the broad initial bubble size distribution and upwelling flows at these seeps. Although smaller bubbles (<1 mm) completely dissolve below ~400 m (150 m above the sea floor), larger bubbles (~>2.4 mm) transport their CH_4 far greater distances, ultimately dissolving near the mixed layer or even surfacing (see Supplementary Fig. S4). As the larger bubbles have a lower surface area to volume ratio and a larger volume, the CH_4 transport efficiency increases with bubble size. Plume aqueous CH_4 produced by small-bubble dissolution is probably diluted by mixing with ambient water between 100 and 300 m where the currents were much stronger. Upwelling flows result from the ensemble buoyancy force of the plume bubbles, and decrease the transit time to the sea surface[15]. The plume spreading-angle is only ~5.2° and the thermocline was locally raised above the plumes in comparison with the background sites (see Supplementary Figs S5–S7), which can be explained only by the vertical transport of deeper water. Thus, we conclude that upwelling flows persist at least to the pycnocline. The increase in methane concentrations above ~80 m is consistent with plume transport of deeper fluids to the pycnocline. As a result of the sharp and large density difference between plume fluids and ambient sea water at this depth, the plume cannot support the deeper fluid, causing detrainment of plume fluids enriched in aqueous CH_4 into the base of the mixed layer. This causes a build-up of CH_4 concentrations as the CH_4 flux into the mixed layer is higher than the air–sea flux. Visual contact with the bubbles was obscured/lost between ~15 and 70 m by turbulence and emptying the submersible's ballast tanks; however, the numerical bubble simulations predict the larger bubbles reach the sea surface (see Supplementary Methods, Fig S4), further increasing the mixed-layer methane concentrations. Although bubble oil coatings at two of the sites would further enhance bubble-mediated CH_4 transport by slowing gas transfer, the numerical bubble simulations predict that it is not requisite (see Supplementary Fig. S4). This conclusion is validated by the elevated mixed-layer CH_4 concentrations in the non-oily plume at GB 425.

Mixed-layer methane concentrations are several orders of magnitude greater than produced locally as a by-product of methylphosphonate decomposition under PO_4-limiting conditions (typically 2–4 nM; refs 17–19), and there is no known pathway for CH_4 production during microbial oil degradation under oxic conditions[20]. Thus, the elevated mixed-layer methane concentrations probably result from limited CH_4 oxidation, enhanced bubble-mediated CH_4 transfer through the water column and the deposition of aqueous CH_4 at the base of the mixed layer.

Both research expeditions occurred during the summer when the average mixed-layer depth in the northern GOM is ~30 m (ref. 21). The summer mixed-layer methane concentrations are 30–954 times saturation (Table 1). From the mixed-layer CH_4 concentrations, the contemporary (on the day of sampling) methane fluxes to the atmosphere were estimated. An explanation of the uncertainties in the CH_4 flux estimates is provided in the Methods section. The contemporary methane fluxes from the plumes were computed to be 197 ± 135 to $6{,}520 \pm 3{,}530$ μmol m^{-2} d^{-1}, and from the background sites they are -0.38 ± 0.34 to 7.0 ± 1.4 μmol m^{-2} d^{-1} (Table 1). In the winter, the mixed layer deepens to ~80 m in the northern GOM (ref. 21), where dissolved CH_4 concentrations are higher (Fig. 2). Given that winter winds are also stronger, the wintertime diffusive fluxes to the atmosphere are probably greater than during the summer. The contemporary GOM diffusive fluxes exceed previous estimates from other deepwater environments by 3–4 orders of magnitude[6–8,17,18,22], and are even 2–3 orders of magnitude greater than fluxes from shallow-water seep areas (<200 m; refs 6–8) (see Supplementary Table S1).

The results of the submersible sampling of deepwater hydrocarbon plumes show that the GOM is not only a region where much of the CH_4 escapes aerobic oxidation in the water column and reaches the sea surface from depths >500 m, but also that diffusive fluxes to the atmosphere above these plumes are among the highest reported so far. For example, they are up to three orders of magnitude greater than diffusive fluxes from shallow-water seeps (<100 m) in the Black Sea (53–200 μmol m^{-2} d^{-1}) and the Sea of Okhotsk (3.2–63 μmol m^{-2} d^{-1}; refs 7, 8), and are even greater than far-field fluxes from the prodigious shallow-water seeps at Coal Oil Point, California (see Supplementary Table S1). Given that previous estimates of CH_4 fluxes to the atmosphere from deepwater seeps relied on hydrocast data, the estimated fluxes presented here are the first reported in close vicinity to bubble plumes; the primary CH_4 transport mechanism. These results highlight the importance of detailed and controlled sampling by submersible and shed light on the significance of deepwater seeps as an atmospheric CH_4 source. On the basis of available SAR imagery, a 53,693 km^2 area offshore Louisiana (3.6% of the GOM surface area) contains ~350 perennial seeps at water depths from 200–2,000 m, each containing 6–12 plumes[9,11,12]. This is a minimum estimate that excludes the non-oily plumes such as the GB 425 plumes. Recent seismic studies and ground-truth observations over a larger area have identified ~5,000 seep sites at water depths >200 m in the northern GOM (ref. 23), and there are probably five times as many seeps at shallower depths[24]. Hence, considering the substantial diffusive fluxes estimated in this study, the GOM is potentially a significant source of fossil (^{14}C-depleted) methane to the atmosphere. It is probable that detailed plume sampling at other active hydrocarbon basins such as the Persian Gulf, Caspian Sea, West African Margin and the Alaska North Slope would yield similar CH_4 fluxes. Thus, a more extensive measurement program including submersible sampling of deepwater plumes in the GOM and other hydrocarbon basins would improve estimates of the natural methane input from the ocean and the contribution of marine seeps to the atmospheric fossil methane burden.

Methods

Water-column samples from the bubble plumes were collected by the *Johnson Sea-Link* research submersible and the CTDs were deployed from R/V *Seward Johnson*, both operated by Harbor Branch, during two research expeditions in 2002 and 2003. The submersible samples were collected immediately adjacent to the bubble plumes (~1–3 m) to ensure that the bubbles were not directly sampled. The sampling interval was every ~20 m, and samples were not collected from the sea surface, but rather >2 m below to ensure that floating oil was not sampled. Samples were collected using a suction tube connected to the manipulator arm. The tube outlet was in the back of the submersible, and samples were directly pumped into serum bottles that were immediately capped and crimped by the observer. Duplicate samples were collected for both methane concentration and isotopic composition, and were poisoned immediately with a saturated $HgCl_2$ solution to halt microbial production and oxidation of methane.

CH_4 and $\delta^{13}C$–CH_4 analyses. C_1–C_3 hydrocarbons were analysed on a gas chromatograph equipped with a flame ionization detector (GC 14A, Shimadzu Corp.). C_1–C_3 compounds were resolved with isothermal 60 °C runs using ultrahigh-purity N_2 as a carrier gas through a 3.658 m by 0.318 cm packed column (*n*-octane Res-Sil C). The standard error of the CH_4 analyses was ±2%. $\delta^{13}C$–CH_4 isotopic analyses were carried out on a Finnigan MAT 252 mass spectrometer with a GC1 interface with a standard deviation of 0.6‰.

Model for water-column methane oxidation. As methane ascends through the water column and is aerobically oxidized, the residual CH_4 becomes isotopically enriched in ^{13}C ($CH_4 + 2O_2 \rightarrow CO_2 + 2H_2O$) with an isotopic fractionation factor (α) of ~1.020. Thus, an increase in $\delta^{13}C$–CH_4 from the sea floor to the sea surface is an indicator of the occurrence and extent of microbial CH_4 oxidation assuming mixing with ambient sea water is negligible. The fractionation factor of 1.020 is the average of published values for aerobic methane oxidation determined in laboratory and field experiments[25,26]. An open-system estimation is probably representative of the plumes sampled in this study, as they have been observed to persist at the same location among multiple SAR images, and thus are perennial[9,11,12] (see Supplementary Fig. S2). This suggests that geologically sourced methane is continuously added to the plumes from focused gas vents, and methane is simultaneously being consumed by microbial oxidation. In the model, it is assumed that methane is added at a constant rate with a constant isotopic signature, mixing with background methane is negligible (see Supplementary Discussion) and the removal of CH_4 is primarily by aerobic oxidation, which is proportional to the amount of CH_4 in the system and is the only pathway for isotope fractionation. With these assumptions, the open-system equation[14] was used:

$$\delta^{13}C_{CH_4}{}^{o} = (f \cdot (\delta^{13}C_{CH_4} + 10^3))/(\alpha - \alpha(1-f)^{1/\alpha}) - 10^3$$

where $\delta^{13}C_{CH_4}{}^{o}$ is the bottom-water methane carbon isotope ratio (equivalent to the vent input ratio), α is the fractionation factor (1.020) and f is the fraction of the input flux of CH_4 to the water column that is oxidized. f was determined iteratively on the basis of the water-column $\delta^{13}C$–CH_4 depth profiles.

Estimation of the gas transfer coefficient k_{avg}. The methane fluxes to the atmosphere were computed using the diffusive exchange equation

$$\text{Flux} = k_{avg}(C_{plume} - C_{eq})$$

where k_{avg} is the gas transfer coefficient at the average wind speed and C_{eq} is the seawater CH_4 concentration in equilibrium with air at ambient conditions[27]. The gas transfer coefficient for the diffusive flux equation was computed using the empirical Wanninkhof [28] relationship.

$$k_{avg} = 0.31u_{avg}^2(Sc/660)^{-0.5}$$

where u_{avg} is the average wind speed at 10 m above the sea surface and Sc is the Schmidt number. Both the equilibrium CH_4 concentration and Sc were computed on the basis of the submersible temperature and salinity profiles at each site (see Supplementary Figs S5 and S6). The wind speeds at the three focus sites were obtained from the National Data Buoy Center Stations 42038 and 42041 (see: http://www.ndbc.noaa.gov/). Station 42038 is located 15 km from the GB 425 mud volcano, and Station 42041 is 100 km from GC 185 and 75 km from GC 234 (Fig. 1c). The average and range in daily and seasonal wind speeds, as well as the calculated k_{avg} at each site is presented in Supplementary Table S2.

Uncertainties in the estimated diffusive CH_4 fluxes arise from inherent variations in u_{avg} affecting the k_{avg} estimation (see Supplementary Table S2), and the various relationships between u_{avg} and k_{avg} in the literature[29]. For instance, an increase in wind speed from 4 to 5 cm s^{-1} (daily average) increases the methane flux estimate by ~50% (ref. 29). In addition, for a given u_{avg}, use of the various other parameterizations for k_{avg} produces differences in the methane flux of 10–40% (ref. 29). Two of the sites sampled have sea-surface oil slicks associated with the plumes, and these surface films can reduce gas exchange by as much as 50% (ref. 30), suggesting the diffusive flux estimates at GC 185 and GC 234 are high values. It should be noted that the sea-surface trajectories of the floating oil are very complicated, and the locations of the slicks are highly variable over short timescales; thus, areas with elevated mixed-layer CH_4 concentrations are not continuously covered with these surface films.

Received 17 July 2008; accepted 9 June 2009; published online 5 July 2009

References

1. Denman, K. L. *et al.* in *IPCC Climate Change 2007: The Physical Science Basis* (eds Solomon, S. D. *et al.*) 499–588 (Cambridge Univ. Press, 2007).
2. Etiope, G., Lassey, K. R., Klusman, R. W. & Boschi, E. Reappraisal of the fossil methane budget and related emission from geologic sources. *Geophys. Res. Lett.* **35**, L09307 (2008).
3. Valentine, D. L., Blanton, D. C., Reeburgh, W. S. & Kastner, M. Water column methane oxidation adjacent to an area of active hydrate dissociation, Eel River Basin. *Geochim. Cosmochim. Acta* **65**, 2633–2640 (2001).
4. Grant, N. J. & Whiticar, M. J. Stable carbon isotopic evidence for methane oxidation in plumes above Hydrate Ridge, Cascadia Oregon Margin. *Glob. Biogeochem. Cycles* **16**, 1124 (2002).
5. McGinnis, D. F., Greinert, J., Artemov, Y., Beaubien, S. E. & Wüest, A. Fate of rising methane bubbles in stratified waters: How much methane reaches the atmosphere? *J. Geophys. Res.* **111**, C09007 (2006).
6. Kessler, J. D. *et al.* Basin-wide estimates of the input of methane from seeps and clathrates to the Black Sea. *Earth Planet. Sci. Lett.* **243**, 366–375 (2006).
7. Yoshida, O., Inoue, Y., Watanabe, S., Noriki, S. & Wakatsuchi, M. Methane in the western part of the Sea of Okhotsk in 1998–2000. *J. Geophys. Res.* **109**, C09S12 (2004).
8. Schmale, O., Greinert, J. & Rehder, G. Methane emission from high-intensity marine gas seeps in the Black Sea into the atmosphere. *Geophys. Res. Lett.* **32**, L07609 (2005).

9. De Beukelaer, S. M. *Remote Sensing Analysis of Natural Oil and Gas Seeps on the Continental Slope of the Northern Gulf of Mexico*. MSc thesis, College Station, Texas A&M Univ. (2003).
10. Leifer, I. & MacDonald, I. Dynamics of the gas flux from shallow gas hydrate deposits: Interaction between oily hydrate bubbles and the oceanic environment. *Earth Planet. Sci. Lett.* **210**, 411–424 (2003).
11. MacDonald, I. R. *et al*. Transfer of hydrocarbons from natural seeps to the water column and atmosphere. *Geofluids* **2**, 95–107 (2002).
12. MacDonald, I. R., Kastner, M. & Leifer, I. Estimates of natural hydrocarbon flux in the Gulf of Mexico basin from remote sensing data. *EGU General Assembly Proc.* abstr. EGU-05-A-09970 (2005).
13. MacDonald, I. R. *et al*. Asphalt volcanism and chemosynthetic life in the Campeche Knolls: Gulf of Mexico. *Science* **304**, 999–1002 (2004).
14. Kessler, J. D., Reeburgh, W. S. & Tyler, S. C. Controls on methane concentration and stable isotope (δ^2H–CH_4 and δ^{13}C–CH_4) distributions in the water columns of the Black Sea and Cariaco Basin. *Glob. Biogeochem. Cycles* **20**, GB4004 (2006).
15. Leifer, I., Luyendyk, B. P., Boles, J. & Clark, J. F. Natural marine seepage blowout: Contribution to atmospheric methane. *Glob. Biogeochem. Cycles* **20**, GB3008 (2006).
16. Rehder, G., Leifer, I., Brewer, P. G., Friederich, G. & Peltzer, E. T. Controls on bubble dissolution inside and outside the hydrate stability field from open ocean field experiments and numerical modeling. *Mar. Chem.* doi: 10.1016/j.marchem.2009.03.004 (2009).
17. Tilbrook, B. D. & Karl, D. M. Methane sources, distributions and sinks from California coastal waters to the oligotrophic North Pacific gyre. *Mar. Chem.* **49**, 51–64 (1995).
18. Holmes, M. E., Sansone, F. J., Rust, T. M. & Popp, B. N. Methane production, consumption, and air–sea exchange in the open ocean: An evaluation based on carbon isotopic ratios. *Glob. Biogeochem. Cycles* **14**, 1–10 (2000).
19. Karl, D. M. *et al*. Aerobic production of methane in the sea. *Nature Geosci.* **1**, 473–478 (2008).
20. Head, I. M., Jones, D. M. & Röling, W. F. M. Marine microorganisms make a meal of oil. *Nature Rev. Microbiol.* **4**, 173–182 (2006).
21. Weatherly, G. Intermediate depth circulation in the Gulf of Mexico: PALACE float results for the Gulf of Mexico between April 1998 to March 2002. *OCS Study MMS 2004-013* (US Department of Interior, Minerals Management Service).
22. Owens, N. J. P., Law, C. S., Mantoura, R. F. C., Burkill, P. H. & Llewellyn, C. A. Methane flux to the atmosphere from the Arabian Sea. *Nature* **354**, 293–296 (1991).
23. Frye, M. *Preliminary Evaluation of in-Place Gas Hydrate Resources: Gulf of Mexico Outer Continental Shelf*. MMS Report 2008-004 (US Department of Interior, Minerals Management Service, 2008).
24. Hovland, M., Judd, A. G. & Burke, R. A. Jr The global flux of methane from shallow submarine sediments. *Chemosphere* **26**, 559–578 (1993).
25. Kinnaman, F. S., Valentine, D. L. & Tyler, S. C. Carbon and hydrogen isotope fractionation associated with the aerobic microbial oxidation of methane, ethane, propane and butane. *Geochim. Cosmochim. Acta* **71**, 271–283 (2007).
26. Sansone, F. J., Popp, B. N., Gasc, A., Rust, T. M. & Graham, A. W. Highly elevated methane in the eastern tropical North Pacific and associated isotopically enriched fluxes to the atmosphere. *Geophys. Res. Lett.* **28**, 4567–4570 (2001).
27. Yamamoto, S., Alcauskas, J. B. & Crozier, T. E. Solubility of methane in distilled water and seawater. *J. Chem. Eng. Data* **21**, 78–80 (1976).
28. Wanninkhof, R. Relationship between wind speed and gas exchange over the ocean. *J. Geophys. Res.* **97**, 7373–7382 (1992).
29. Mau, S. *et al*. Dissolved methane distributions and air–sea flux in the plume of a massive seep field, Coal Oil Point, California. *Geophys. Res. Lett.* **34**, L22603 (2007).
30. Frew, N. M. *et al*. Air–sea gas transfer: Its dependence on wind stress, small-scale roughness, and surface films. *J. Geophys. Res.* **109**, C08S17 (2004).

Acknowledgements

We thank the crew members and pilots of the R/V *Seward Johnson* and *Johnson Sea-Link* for their support in meeting the objectives of the 2002 and 2003 dive programs. We thank D. Valentine for use of his laboratory for the C_1–C_3 hydrocarbon analyses, and F. Kinnaman, B. Deck, R. Solem and T. Rust for technical assistance. We greatly appreciate the shipboard assistance from G. Robertson and the numerous UCSD and Texas A&M students during the 2002 and 2003 research expeditions. J. Kessler and J. Greinert are thanked for constructive comments, which helped improve the manuscript. Research financial support was provided by the US Department of Energy National Methane Hydrates R&D Program.

Author contributions

E.A.S. carried out the chemical analyses and the methane oxidation/diffusive flux calculations, evaluated the results and wrote the manuscript. M.K., I.R.M. and E.A.S. oversaw the two field campaigns and sample acquisition. The numerical bubble propagation simulations were conducted by I.L. All authors provided valuable comments on the manuscript.

Additional information

Supplementary information accompanies this paper on www.nature.com/naturegeoscience. Reprints and permissions information is available online at http://npg.nature.com/reprintsandpermissions. Correspondence and requests for materials should be addressed to E.A.S.